

Folding Polyiamonds into Octahedra

EVA STEHR
eva@stehr.dev
TU Braunschweig

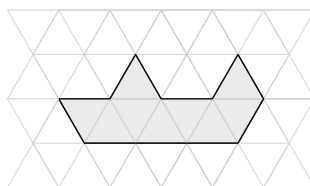
LINDA KLEIST
kleist@ibr.cs.tu-bs.de
TU Braunschweig

July 2022

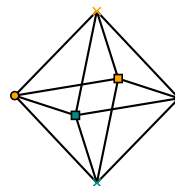
We study polyiamonds (polygons arising from the triangular grid) that fold into the smallest yet unstudied platonic solid – the octahedron. We show a number of results. Firstly, we characterize foldable polyiamonds containing a hole of positive area, namely each but one polyiamond is foldable. Secondly, we show that a convex polyiamond folds into the octahedron if and only if it contains one of five polyiamonds. We thirdly present a sharp size bound: While there exist unfoldable polyiamonds of size 14, every polyiamond of size at least 15 folds into the octahedron. This clearly implies that one can test in polynomial time whether a given polyiamond folds into the octahedron. Lastly, we show that for any assignment of positive integers to the faces, there exist a polyiamond that folds into the octahedron such that the number of triangles covering a face is equal to the assigned number.

1 Introduction

Algorithmic origami is a comparatively young branch of computer science that studies the algorithmic aspects of folding various materials. The construction of three-dimensional objects from two-dimensional raw materials is of particular interest and has applications in robotics in general [11, 13], and also in the construction of objects in space [9].



(a) A polyiamond P .



(b) The octahedron \mathcal{O} .

Figure 1: Does the polyiamond P fold into the octahedron \mathcal{O} ?

While foldings of polycubes and tetrahedra have already been studied, we take the next step and focus on the question of whether a given polyiamond folds into the octahedron, e.g., does the polyiamond in Figure 1 fold into the octahedron?

Terminology By the *octahedron* \mathcal{O} , we refer to the regular octahedron composed of eight equilateral (unit) triangles; for an illustration consider Figure 1(b). Note that four triangles meet in each of the six corners of the octahedron. Because all faces of the octahedron are triangles, our pieces of paper are polygons arising from the triangular grid. A *polyiamond* of size n is a connected polygon in the plane formed by joining n triangles from the triangular grid by identifying some of their common sides; for an example consider Figure 1(a). To avoid confusion with the corners of the octahedron, we refer to the vertices of the triangles forming P as the *vertices* of P ; note that these vertices may also lie inside P .

We view P as a set which includes the n open triangles and a subset of the unit-length boundary edges shared by any two of these triangles; the existence of such an edge models the fact that the two incident triangles are glued along this side. Because we only want robust connections between triangles via their sides, we do not specify the existence or non-existence of vertices which do not influence the foldability. However, for the upcoming definitions of slits and holes, we assume that the vertices do not belong to the polyiamond.

If a shared edge does not belong to P , we call it a *slit edge*. We also allow the polyiamonds to have holes; a *hole* of a polyiamond is a bounded connected component of its complement, which is different from a single vertex. We call a hole a *slit* if it has area zero and consists of one or more slit edges. We consider two polyiamonds to be *the same* if they are congruent, i.e., if they can be transformed into one another by a set of translations, rotations and reflections. Moreover, a polyiamond is *convex* if it forms a convex set in the plane (after adding a finite set of points corresponding to vertices).

Folding model We consider foldings in the *grid folding model*, where folds along the grid lines are allowed such that in the final state every triangle covers a face of the octahedron, i.e., we forbid folding material strictly outside or inside the octahedron. Consequently, in the final state the folding angles are $\pm\beta := \arccos(1/3)$ or $\pm 180^\circ$. Moreover, a folding of a polyiamond P into the octahedron \mathcal{O} induces a *triangle-face-map*, i.e., a mapping of the triangles of P to the faces of \mathcal{O} . We say P *folds into* \mathcal{O} (or P *is foldable*), if P can be transformed by folds along the grid lines into a folded state such that the induced triangle-face-map is surjective, i.e., each face of \mathcal{O} is covered by at least one triangle. In order to study non-foldable polyiamonds, we also consider partial foldings, i.e., foldings where potentially not all faces of \mathcal{O} are covered. Note that partial foldings induce triangle-face-maps that are not necessarily surjective.

1.1 Related work

Past research has particularly focused on folding polyominoes into *polycubes*. Allowing for folds along the *box-pleat grid* (consisting of square grid lines and alternating diagonals),

Benbernou et al. (with differing co-authors) show that every polycube Q of size n can be folded from a sufficiently large square polyomino [6] or from a $2n \times 1$ strip-like polyomino [5]. Moreover, common unfoldings of polycubes have been investigated in the grid model. The (*square*) *grid model* allows folds along the grid lines of a polyomino with fold angles of $\pm 90^\circ$ and $\pm 180^\circ$, and allows material only on the faces of the polyhedron. Benbernou et al. show that there exist polyominoes that fold into all polycubes with bounded surface area [5] and Aloupis et al. study common unfoldings of various classes of polycubes [4]. Moreover, there exist polyominoes that fold into several different boxes [1, 12, 14, 15, 16].

Decision questions for folding (unit) cubes are studied by Aichholzer et al. [2, 3]. The *half-grid model* allows folds of all degrees along the grid lines, the diagonals, as well as along the horizontal and vertical halving lines of the squares. In this model, every polyomino of size at least 10 folds into the cube [3]. The remaining polyominoes of smaller size are explored by Czajkowski et al. [8]. In the grid model, Aichholzer et al. [3] characterized the foldable tree-shaped polyominoes that fit within a $3 \times n$ strip. Investigating polyominoes with holes, Aichholzer et al. [2] show that all but five *basic* holes (a single unit square, a slit of length 1, a straight slit of length 2, a corner slit of length 2 and a U-shaped slit of length 3) guarantee that the polyomino folds in the grid model into the cube.

In the context of polyiamonds, Aichholzer et al. [3] present a nice and simple characterization of polyiamonds that fold into the smallest platonic solid: Even when restricting to folds along the grid lines, a polyiamond folds into the tetrahedron if and only if it contains one of the two tetrahedral nets.

Results and organization In this work, we study foldings to the smallest yet unstudied platonic solid – the octahedron. Our main results are as follows:

- In Section 2, we identify some sufficient and necessary conditions for foldability and take a closer look at polyiamonds with slits and holes.
- Among our findings in Section 3, we characterize foldable polyiamonds containing a hole of positive area: each but one polyiamond is foldable.
- In Section 4, we characterize the convex foldable polyiamonds: A convex polyiamond folds into \mathcal{O} if and only if it contains one of five polyiamonds.
- In Section 5, we show that every polyiamond of size ≥ 15 is foldable. A non-foldable polyiamond of size 14 proves that this bound is best possible. We highlight that an analogous statement for folding polyominoes into cubes does not exist in the grid folding model, i.e., there exist arbitrarily large polyominoes that do not fold into the cube. For instance, large rectangular polyominoes [2, Corollary 2].
- In Section 6, we discuss the reverse question: For an assignment of positive integers to the faces of the octahedron \mathcal{O} , does there exist a polyiamond that folds into \mathcal{O} such that the number of triangles covering each face is equal to the assigned number? We prove that such a polyiamond exists for any such assignment.

2 Some Tools

In this section, we present tools for proving or disproving the foldability of a polyiamond into an octahedron. Firstly, we present a useful connection between 3-colorings of the triangular grid and polyiamonds inheriting the vertex coloring that are folded into the octahedron. As indicated in Figure 2, the triangular grid graph allows for a proper 3-coloring. Because every (connected) inner triangulation has at most one 3-coloring (up to exchange of the colors), every polyiamond has a unique 3-coloring which is induced by the triangular grid. If there exists a slit edge along a grid line, the polyiamond graph may have several vertices corresponding to one grid vertex, see also Figure 7(b). Note that each corner of \mathcal{O} has a unique non-adjacent corner which we call its *antipodal*.

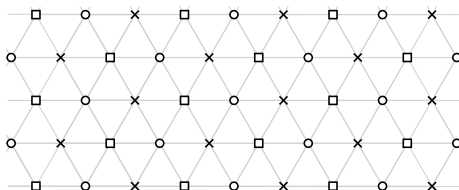


Figure 2: A 3-coloring of the triangular grid.

In order to study the non-foldability, we also consider partial foldings. In particular, when relaxing the condition that all faces are covered, we say a polyiamond is *partially* folded into the octahedron.

Lemma 1. *Let P be a polyiamond with a 3-coloring of its vertices. In every (partial) folding of P to the octahedron \mathcal{O} , the vertices of each color class are mapped to (one corner or a pair of) antipodal corners of \mathcal{O} .*

Proof. Consider two neighboring triangles of P and note that their two private vertices have the same color. If their common side is folded by $\pm\beta$, these two vertices are mapped to antipodal corners of \mathcal{O} ; otherwise the edge is folded by $\pm 180^\circ$ and the two vertices are mapped to the same corner of \mathcal{O} . The fact that P is connected implies that every color class is mapped to a different set of antipodal corners. \square

We repeatedly use Lemma 1 in order to disprove foldability. Moreover, for folded polyiamonds, Lemma 1 allows to illustrate the mapping of vertices to corners of \mathcal{O} by vertex colorings where antipodal corners of \mathcal{O} are represented by the same shape but different colors, for an example consider Figure 4. Clearly, such a vertex coloring induces a triangle-face map.

2.1 Foldability

A polyiamond P *contains* a polyiamond P' if P' can be translated, rotated, and reflected such that all triangles and triangle sides of P' also belong to P . Restricting our attention to the triangles, a polyiamond P \triangle -*contains* a polyiamond P' if all triangles of P' belong to P . For example, the polyiamond in Figure 7(b) does not contain but \triangle -contains the

polyiamond in Figure 7(a). As we will see in Observation 5, neither containment nor Δ -containment of a foldable polyiamond is a sufficient folding criterion. Nevertheless, we are able to show two sufficient criteria based on Δ -containment of foldable polyiamonds. By zig-zag-folding as indicated in Figure 3, every polyiamond can be reduced to a contained convex polyiamond.

Lemma 2. *A polyiamond P is foldable if it Δ -contains a convex foldable polyiamond C .*

Proof. Firstly, we reduce P to C : For every boundary side s of C , we fold the triangles of P outside C in a zig-zag-manner. To this end, we fold along the grid lines parallel to s with $+180^\circ$ and -180° folds alternatingly, as illustrated in Figure 3.

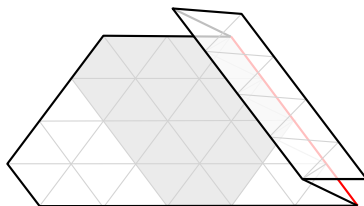


Figure 3: Folding strategy to reduce a polyiamond to a convex subpolyiamond by zig-zag-folding the outside.

As a result, the supporting line of s bounds the folded polyiamond. Because C is convex and contained in P , P can be transformed to C with the above procedure. Secondly, we use the fact that C folds into \mathcal{O} . \square

A *net* of a polyhedron is formed by cutting along certain edges and unfolding the resulting connected set to lie flat without intersections. Nets of the octahedron are depicted in Figure 4. There exist two interesting facts for nets of three-dimensional

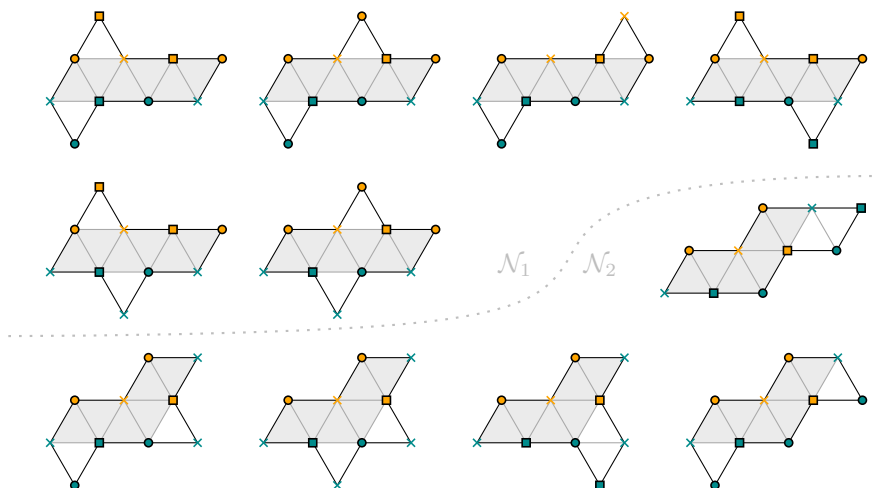


Figure 4: The eleven nets of the octahedron split into two groups \mathcal{N}_1 and \mathcal{N}_2 .

regular convex polyhedra [7]: Firstly, each net is uniquely determined by a spanning tree of the 1-skeleton of the polyhedron, i.e., the cut edges form a spanning tree of the vertex-edge graph. Secondly, dual polyhedra (e.g., the cube and the octahedron) have the same number of nets. Consequently, there exist eleven octahedron nets.

We show that Δ -containing a net is a sufficient folding criterion for a polyiamond.

Lemma 3. *A polyiamond is foldable if it Δ -contains an octahedron net.*

Proof. We partition the set of nets into two groups \mathcal{N}_1 and \mathcal{N}_2 as illustrated in Figure 4. Note that within each group, the vertex-corner-maps (can be shifted such that they) are consistent on common triangles. For $i = 1, 2$, we consider the smallest convex polyiamond S_i containing the nets of \mathcal{N}_i as depicted in Figure 5. The coloring of the vertices gives a mapping to the corners of \mathcal{O} and thus describes a folding of S_i into \mathcal{O} .



Figure 5: Illustration for the proof of Lemma 3.

By Lemma 2, all polyiamonds that contain a convex polyiamond can be reduced to the convex polyiamond. By construction, not all triangles of S_i are present in each net of \mathcal{N}_i . However, each net has at least eight triangles with pairwise different labels. The non-existence of a triangle harms the foldability only if it is essential to cover a face. \square

2.2 Non-foldability

The following lemma is a crucial tool to disprove foldability. To this end, let C_6 and C_{10} denote the polyiamonds depicted in Figures 6(a) and 6(c), respectively.

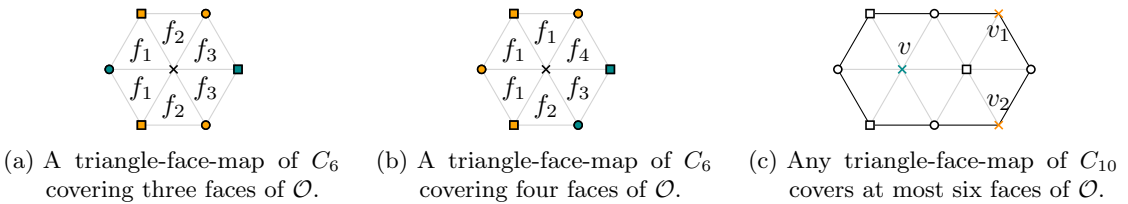


Figure 6: Illustration of Lemma 4 and its proof.

Lemma 4. *Let P be a polyiamond (partially) folded into the octahedron \mathcal{O} .*

(i) *Every C_6 that is Δ -contained in P covers at most four different faces of \mathcal{O} .*

- (ii) If a C_6 in P covers exactly three or four faces, then the induced triangle-face-mapping is unique (up to symmetry) and as depicted in Figures 6(a) and 6(b), respectively.
- (iii) Every C_{10} contained in P covers at most six different faces of \mathcal{O} .

Proof. Let v denote the central vertex of C_6 . In the folded state, v is mapped to a corner c of the octahedron which is (like every corner) incident to four faces.

- (i) Because every triangle of C_6 is incident to vertex v , these triangles cover a subset of the four faces incident to c .
- (ii) We consider a 3-coloring as indicated in Figure 6(a). If all circle or all square vertices map to a same corner, then C_6 covers at most two faces of \mathcal{O} , namely the ones incident to the cross and circle vertex. Hence, if P covers three or four faces, then exactly two vertices of each class map to the same corner and the third vertex of each class maps to its antipodal, we call this vertex *lonely*. We distinguish whether the two lonely vertices are a) adjacent or b) opposite in C_6 , see Figures 6(a) and 6(b). It follows that the number of covered faces is three and four, respectively.
- (iii) We consider a 3-coloring of C_{10} as illustrated in Figure 6(c) and use the fact that each color class is mapped to antipodal corners by Lemma 1. We denote the three cross vertices by v, v_1, v_2 as illustrated in Figure 6(c); similarly, we denote the corner of \mathcal{O} to which v is mapped by c . If at most one v_i (which are both incident to only two triangles) is mapped to the antipodal corner \bar{c} of c , then at most two faces incident to \bar{c} can be covered. If both v_1 and v_2 are mapped to \bar{c} , then the four incident triangles of \bar{c} share a common edge. Consequently, they may cover at most two incident faces. In other words, in both cases at least two faces (incident to \bar{c}) remain uncovered and thus a C_{10} covers at most six faces.

This completes the proof. □

3 On Slits and Holes

In this section, we consider polyiamonds with slits and holes. First of all, we remark that removing individual edges from a foldable polyiamond does not destroy its foldability as long as connectivity is maintained. This allows us to focus on polyiamonds without slit edges, i.e., *sealing* slit edges may only increase the level of difficulty to prove foldability. On the other hand, we note that slits may in fact enable foldability.

Observation 5. *Let P be a polyiamond (Δ -)containing a foldable polyiamond P' . Then, the polyiamond P may not be foldable.*

As we show in Claim 7.4 in the proof of Theorem 7, the polyiamond P in Figure 7(a) does not fold into \mathcal{O} , while the polyiamond P' with additional slit edges in Figure 7(b) can be transformed into a polyiamond Δ -containing a net. Hence, P' is foldable by Lemma 3.

We now characterize foldable polyiamonds with holes of positive area. Let \mathcal{O} denote the polyiamond illustrated in Figure 8(d).

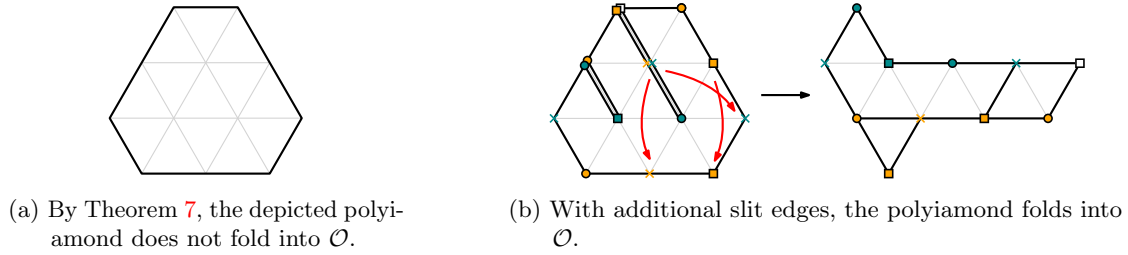


Figure 7: Illustration for Observation 5.

Theorem 6. *Let P be a polyiamond containing a hole h of positive area. Then P folds into \mathcal{O} if and only if it is not the polyiamond O .*

Proof. The non-foldability of O is analogous to the proof that the polyiamond depicted in Figure 7(a) is non-foldable, see Claim 7.4 below.

For the reverse direction, we focus on a largest hole h with positive area and distinguish two cases:

If h contains two neighboring triangles, then we reduce P to the polyiamond P_c depicted in Figure 8(c) as follows: we choose two neighboring triangles of h which form a (potentially smaller) hole h' in the form of a parallelogram. Then, we fold all triangles that do not touch h' with a vertex or edge by zig-zag-folding the outside as in Figure 3. This results in the polyiamond P_c because h and thus h' are enclosed by a cycle of triangles of P . Moreover, it is easy to check that P_c is foldable, e.g., when inducing the triangle-face-map depicted in Figure 8(c).

It remains to consider the case that h contains exactly one triangle and P is not O . If P can be reduced (by zig-zag-folding) to the polyiamond P_a depicted in Figure 8(a), then P folds into \mathcal{O} by Lemma 2. Otherwise, we use zig-zag-folds to obtain a subpolyiamond P' of P_b depicted in Figure 8(b). Because P is different from O and cannot be reduced to P_a , this ensures that P' has at least one triangle with label f_8 . Because P_b folds into \mathcal{O} , so does P . \square

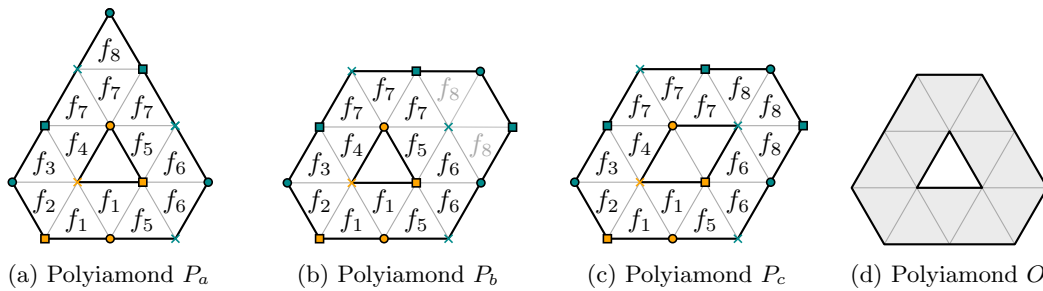


Figure 8: illustration for the proof of Theorem 6.

4 Characterization for Convex Polyiamonds

In this section, we characterize convex foldable polyiamonds. Let \mathcal{C} denote the set of five convex polyiamonds depicted in Figure 9.

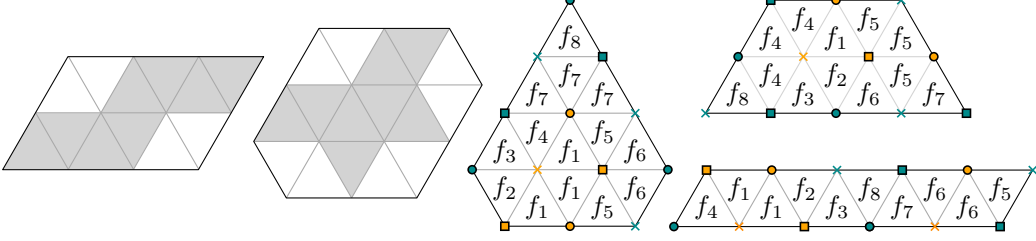


Figure 9: Illustration for Theorem 7; the set \mathcal{C} of foldable polyiamonds and their foldings.

Theorem 7. *A convex polyiamond P folds into \mathcal{O} if and only if it contains one of the five polyiamonds in \mathcal{C} .*

Proof. First, we show that a convex polyiamond P folds into \mathcal{O} if it (Δ -)contains a polyiamond in \mathcal{C} . Note that each polyiamond in \mathcal{C} is convex. Hence, by Lemma 2, it suffices to present folding strategies for the polyiamonds in \mathcal{C} , see Figure 9. While two polyiamonds contain an octahedral net, we present explicit strategies for the remaining three.

Second, we show that every convex polyiamond that folds into \mathcal{O} contains a polyiamond from \mathcal{C} . To do so, we construct all convex \mathcal{C} -free polyiamonds, i.e., all convex polyiamonds that contain none of the five polyiamonds in \mathcal{C} . The construction is as follows, for an illustration consider Figure 10:

We start with the unique polyiamond of size 1. Then, we consider all possibilities to enlarge every constructed polyiamond by one triangle and extend it to the smallest convex polyiamond containing it, i.e., we add just enough triangles such that the resulting polyiamond is convex again. We stop when we encounter a polyiamond from \mathcal{C} or a polyiamond containing one of them.

By their convexity and Lemma 2, it suffices to show the non-foldability of the inclusion-wise maximal \mathcal{C} -free polyiamonds. The construction shows that the set $\bar{\mathcal{C}}$ of inclusion-wise maximal \mathcal{C} -free polyiamonds consists of the four polyiamonds $\bar{\mathcal{C}}_1 := o$, $\bar{\mathcal{C}}_2 := w$, $\bar{\mathcal{C}}_3 := s$, and $\bar{\mathcal{C}}_4 := p$, i.e., each \mathcal{C} -free polyiamond is contained in some polyiamond in $\bar{\mathcal{C}}$. It remains to show that all of these do not fold into \mathcal{O} .

Claim 7.1. *The polyiamond $\bar{\mathcal{C}}_1$ does not fold into \mathcal{O} .*

The polyiamond $\bar{\mathcal{C}}_1$ contains a C_6 , see Figure 11(a). By Lemma 4(i), the contained C_6 covers at most four faces of the octahedron \mathcal{O} . Hence, in every partial folding of $\bar{\mathcal{C}}_1$ into \mathcal{O} , $\bar{\mathcal{C}}_1$ covers at most seven faces of \mathcal{O} . Consequently, it does not fold into \mathcal{O} .

Claim 7.2. *The polyiamond $\bar{\mathcal{C}}_2$ does not fold into \mathcal{O} .*

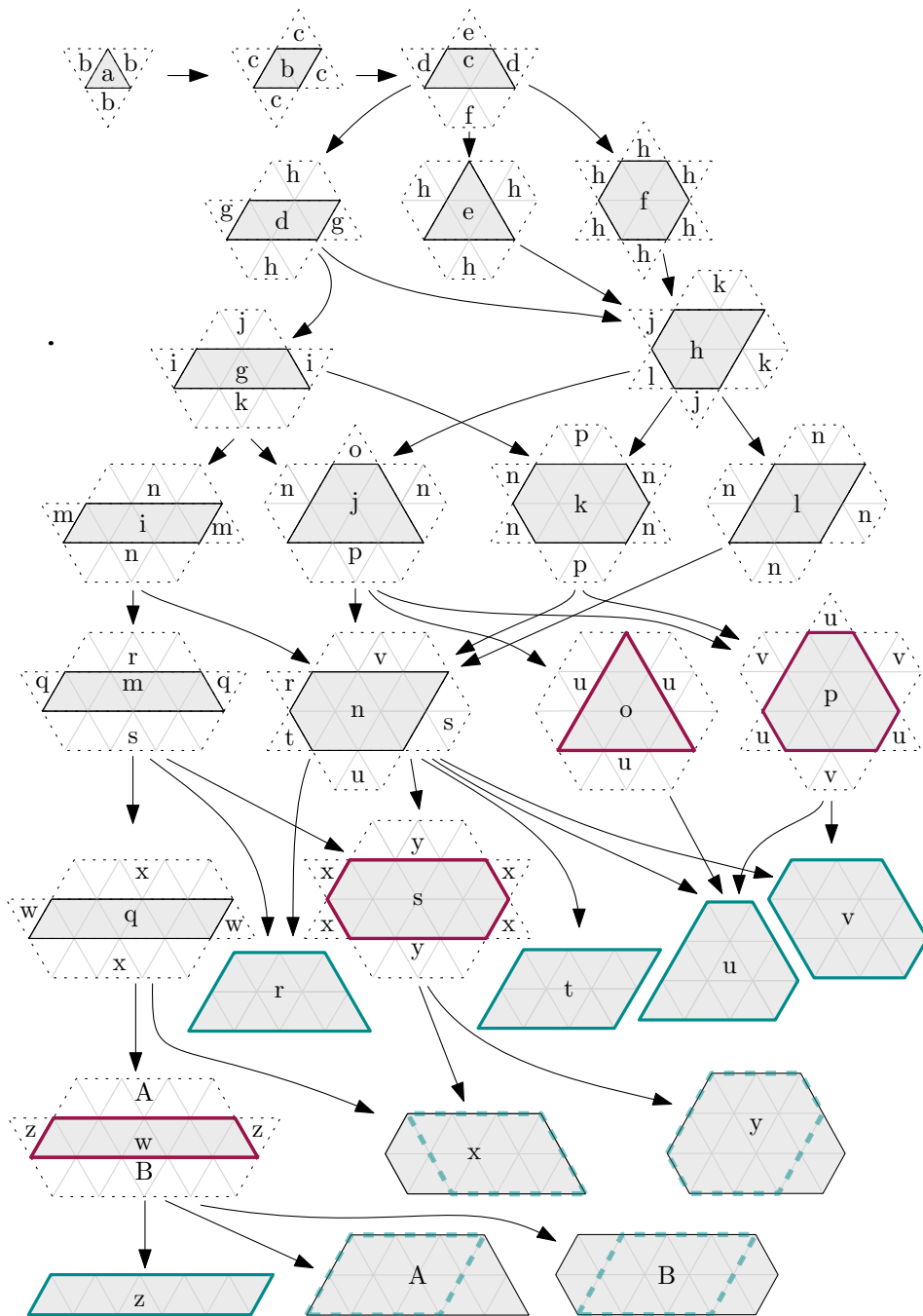


Figure 10: Construction of all \mathcal{C} -free polyiamonds; the inclusion-wise maximal \mathcal{C} -free polyiamonds o , p , s , and w are highlighted in red.

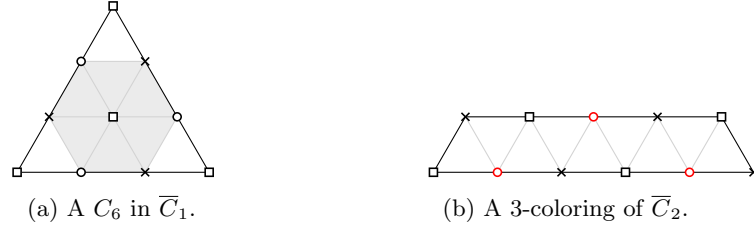


Figure 11: Illustration for the proof that \overline{C}_1 and \overline{C}_2 do not fold into \mathcal{O} .

For the purpose of a contradiction, we assume that \overline{C}_2 does fold into \mathcal{O} . We consider a 3-coloring as illustrated in Figure 11(b) and use the fact that each color class is mapped to a pair of antipodal pairs by Lemma 1. Note that there exist only three circle vertices, each of which is adjacent to three faces of \overline{C}_2 . Hence, one (of the two antipodal) corner of \mathcal{O} is covered by only one circle vertex implying that not all of its incident faces are covered.

Claim 7.3. *The polyiamond \overline{C}_3 does not fold into \mathcal{O} .*

The polyiamond \overline{C}_3 can be viewed as copies of C_6 and C_{10} overlapping in two triangles, see Figure 12(a). For the purpose of a contradiction, we consider a 3-coloring of \overline{C}_3 as illustrated in Figure 12(b). Note that there are four square vertices in total; we denote them by v_1, v_2, v_3, v_4 . Moreover, the three leftmost square vertices cannot all map to the same corner c ; otherwise the left C_6 maps to at most two faces and \overline{C}_3 covers at most $2 + 6 - 1 = 7$ faces. We distinguish two cases.

If v_2 and v_3 are mapped to c (and v_1 to the antipodal corner \bar{c}), then all of their six incident triangles contain one of two neighboring edges of c ; for an illustration consider Figure 12(b). Hence, they cover at most three faces incident to c . Moreover, v_4 must map to \bar{c} ; otherwise the two triangles incident to v_1 are the only ones mapping to any of the four faces incident to \bar{c} . Consequently, all remaining triangles map to a face incident to \bar{c} and thus, they are not able to cover the remaining face incident to c . A contradiction.

It remains to consider the case that v_2 and v_3 are mapped to two antipodal corners c and \bar{c} , respectively. We may assume without loss of generality that v_1 is mapped to the corner c as illustrated in Figure 12(c). Then v_4 is mapped to the antipodal \bar{c} ; otherwise not all faces of \bar{c} are covered. Consequently, all triangles incident to c are incident to v_1 and v_2 . However, four (of the five) triangles incident to v_1 and v_2 share one edge

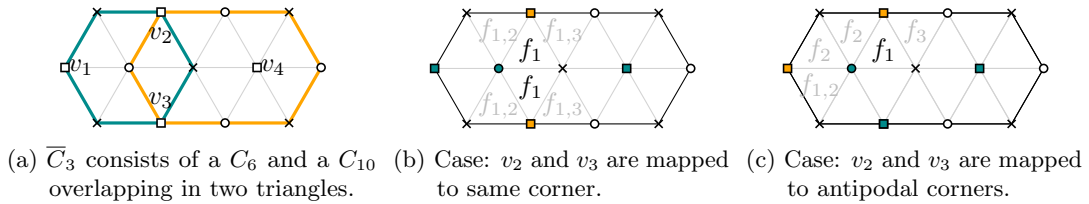


Figure 12: Illustration for the non-foldability of \overline{C}_3 .

of \mathcal{O} . Hence the five triangles of v_1 and v_2 cover at most three faces incident to c . A contradiction to the foldability of \overline{C}_3 .

Claim 7.4. *The polyiamond \overline{C}_4 does not fold into \mathcal{O} .*

The polyiamond \overline{C}_4 consists of a C_{10} and a C_6 overlapping in three triangles as illustrated in Figure 13(a). If their intersection is mapped to three different faces of \mathcal{O} , then by Lemma 4(i) and (iii), \overline{C}_4 covers at most $4 + 6 - 3 = 7$ faces of \mathcal{O} . Consequently, in every folding of \overline{C}_4 into \mathcal{O} , the triangles in the considered intersection map to at most two distinct faces. In the following, we focus on the four central triangles of \overline{C}_4 . By the above observation and the rotational symmetry of \overline{C}_4 , the triangles of each ‘line’ are mapped to at most two distinct faces. We distinguish two cases.

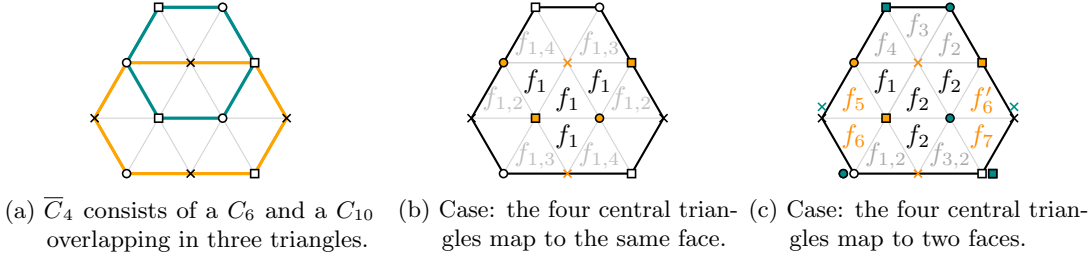


Figure 13: Illustration for the non-foldability of \overline{C}_4 .

If all four triangles map to the same face, denoted by f_1 , then consider Figure 13(b). By their common edge incident to f_1 , each of the two triangles with label $f_{1,i}$ Figure 13(b), $i \in \{2, 3, 4\}$, cover at most one face different from f_1 . Consequently, at most seven faces can be covered in total and this case does not yield a folding of \overline{C}_4 into \mathcal{O} .

If the four central triangles map to two different faces, then by Lemma 1, the map is as illustrated in Figure 13(c). By Lemma 4(i) and (iii), the copy of C_6 covers at most four faces and the copy of C_{10} covers at most six faces. Subtracting the double count of the intersection, the triangles of \overline{C}_4 cover at most $4 + 6 - 2 = 8$ faces. Hence, by Lemma 4(ii), the top copy of C_6 covers exactly four faces and is consistent with the triangle-face-map of Figure 6(b). Note that the two triangles with label $f_{i,2}$, $i \in \{1, 3\}$, in Figure 13(c) contain the common edge of f_i and f_2 and thus they may not cover new faces of \mathcal{O} . It follows that the remaining four triangles cover distinct and new faces of \mathcal{O} . However, this implies that triangles f_6 and f'_6 are mapped to the same face. A contradiction. Hence, \overline{C}_4 does not fold into \mathcal{O} . \square

5 A Sharp Size Bound

As shown in Claim 7.3, the polyiamond \overline{C}_3 is not foldable, i.e., there exist polyiamonds of size 14 that do not fold into \mathcal{O} . In this section, we show the following complementing theorem.

Theorem 8. *Every polyiamond P of size ≥ 15 folds into \mathcal{O} .*

To present an idea of the proof, we give some useful sufficient conditions and a simple upper bound. Let P be a polyiamond and ℓ some grid line. The ℓ -width of P denotes the size of the polyiamond obtained by folding all edges parallel to ℓ in a zig-zag-manner as indicated in Figure 3. The *width* of P is the maximum of the three different ℓ -widths. Because the convex polyiamond $P_- := z$, depicted in Figure 10, folds into \mathcal{O} , we obtain the following.

Lemma 9. *Every polyiamond P of width at least 10 folds into \mathcal{O} .*

Proof. Because P has width 10, it can be folded into the polyiamond P_- by zig-zag-folds. Then, by Theorem 7, P_- can be folded into \mathcal{O} . \square

Moreover, we determine an upper bound on the size of polyiamonds of width ≤ 9 . In particular, they have size ≤ 42 which yields a nice and simple upper bound.

Corollary 10. *Every polyiamond of size > 42 folds into \mathcal{O} .*

Proof. Let P be a polyiamond that does not fold into \mathcal{O} . Then, by Lemma 9, P has width ≤ 9 . Consequently, P is contained in the intersection of three strips of width 9 with different rotation. As illustrated in Figures 14(a) and 14(b), two of these infinite

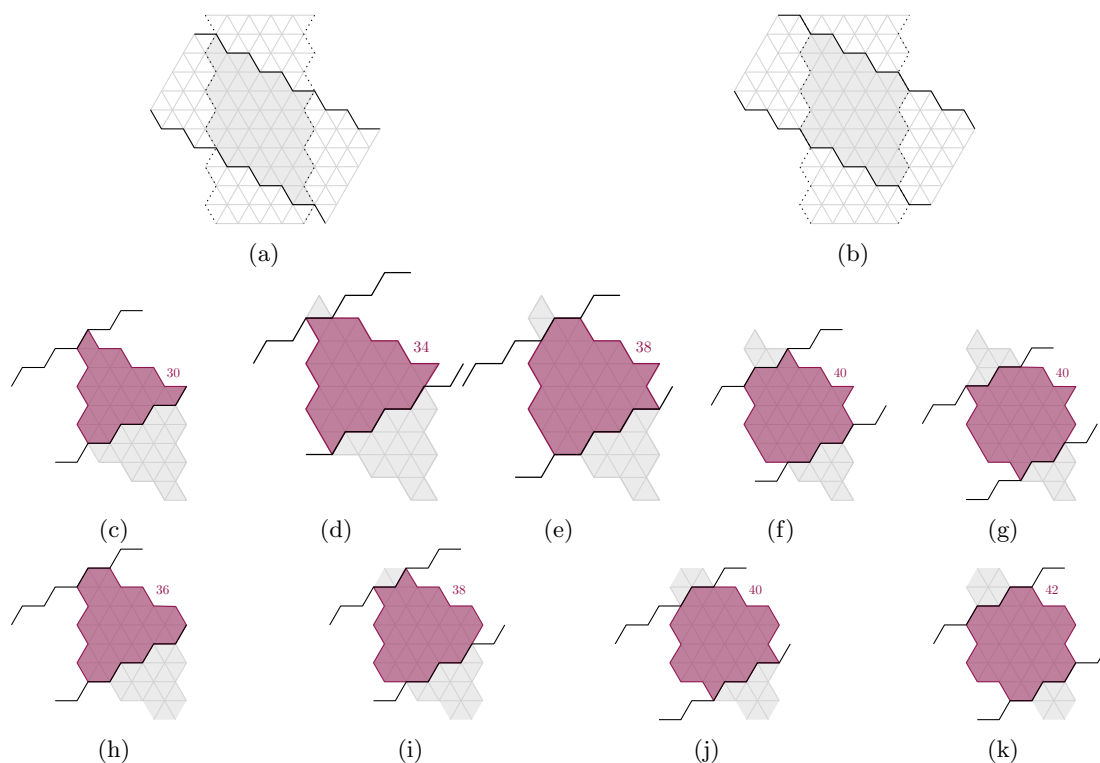


Figure 14: Illustration for the proof of Corollary 10. Construction of the maximal polyiamonds of width ≤ 9 ; their sizes are indicated by numbers.

strips may intersect in two distinct ways. The intersection with different translations of a third strip results in nine polyiamonds (six of which are pairwise different), see Figure 14.

The largest of these polyiamonds has size 42 and is depicted in Figure 14(k). Because P is contained in one of them, P has size at most 42. Consequently, any larger polyiamond is foldable. \square

To show the sharp bound, we need to work a little harder. In particular, the proof is computer-aided.

Proof of the sharp upper bound Theorem 8 is based on a strong sufficient criterion. Let P_X , P_U , P_Z , and P_L denote the polyiamonds depicted in Figures 15(a) to 15(d), respectively. In a first step, we show that polyiamonds that are large enough and do contain one of the four polyiamonds fold into \mathcal{O} .



Figure 15: Illustration of the four polyiamonds used in Lemma 11.

Lemma 11. *Every polyiamond P that \triangle -contains P_X , P_U , P_Z , or P_L and has size ≥ 15 folds into \mathcal{O} .*

Before proving Lemma 11, we show how to deduce Theorem 8.

Theorem 8. *Every polyiamond P of size ≥ 15 folds into \mathcal{O} .*

Proof. We call a polyiamond \mathcal{P} -free if it does not \triangle -contain any of the polyiamonds P_+ , P_X , P_U , P_Z , or P_L . By Theorem 7 and Lemma 11, it remains to show that no \mathcal{P} -free polyiamond of size ≥ 15 exists. To do so, we construct all \mathcal{P} -free polyiamonds bottom-up and show that indeed there exists no such polyiamond. The construction is similar to the one in the proof of Theorem 7: We start with the polyiamond of size 1. Then, we enlarge every \mathcal{P} -free polyiamond of size k by individual triangles and check if the resulting polyiamonds remain \mathcal{P} -free. In this way, we obtain a list of \mathcal{P} -free polyiamonds of size $k + 1$. Table 1 presents the numbers $p(n)$ of \mathcal{P} -free polyiamonds with size n ; these numbers have been generated by computer-search. The code is available at <https://github.com/dasnessie/folding-polyiamonds/>. \square

Table 1: The number $p(n)$ of \mathcal{P} -free polyiamonds of size n .

n	2	3	4	5	6	7	8	9	10	11	12	13	14	15
$p(n)$	1	1	3	4	10	16	22	22	16	9	3	1	0	0

It remains to prove Lemma 11. We split its proof into four claims. Together, Claims 11.1 to 11.4 imply Lemma 11.

Claim 11.1. *Every polyiamond P that \triangle -contains P_X and has size ≥ 15 folds into \mathcal{O} .*

Proof. We consider the C_{10} -frame containing P_X as illustrated in Figure 16(a) and call each connected group of rose triangles a *flap* of P_X . We consider the following cases:

If triangles exist in two distinct flaps, then there exists a triangle-face-map such that some triangles are mapped to (the two missing faces) f_7 and f_8 , see Figure 16(a) (or its mirror image). First, we fold away all (but at most two) triangles that are not contained in the two flaps. The two corner triangles between two flaps may remain. Its foldability is implied by the fact that the polyiamond in Figure 16(a) folds into \mathcal{O} .

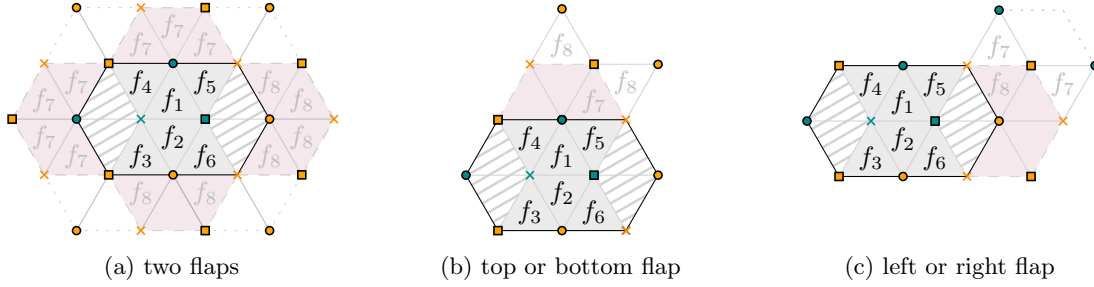


Figure 16: Illustration of the proof of Claim 11.1.

It remains to consider the case that P without C_{10} is attached via only one flap. Because P has size at least 15 and each flap has size at most 4, there exists a triangle outside the flap. Figures 16(b) and 16(c) shows that this guarantees foldability in all cases. \square

Claim 11.2. *Every polyiamond P that \triangle -contains P_U and has size ≥ 15 folds into \mathcal{O} .*

Proof. We may assume that P does not \triangle -contain C_{10} (which \triangle -contains P_X); otherwise Claim 11.1 implies the statement. Consequently, P has six triangles outside the C_{10} -frame containing P , see Figure 17(a). We distinguish two cases: a) there exists a triangle in some flap with a neighboring triangle outside the flap or b) all triangles of P lie within the flaps.

In case a), the map in Figure 17(a) can be reflected (horizontally) such that there exist triangles with labels f_7 and f_8 . The label $f_{7,8}$ indicates that it can be adjusted as wished. Moreover, P folds into \mathcal{O} by some strategy presented in Figure 17(a) (after reducing to a crucial convex subpolyiamond).

In case b), unless all triangles lie within the left and right flap, the map in Figure 17(a) can be reflected such that there exist faces with labels f_7 and f_8 . Moreover, P folds into \mathcal{O} by the strategy presented in Figure 17(a).

If all triangles lie within the left and right flap, we consider the strategy indicated in Figure 17(b). By symmetry, we may assume that the left flap contains at least three triangles. Hence, there exist faces with label f_6 and f_8 ; moreover, a triangle with label f_7 exists in the right flap. As the polyiamond in Figure 17(b) folds into \mathcal{O} , P does as well. This completes the proof. \square

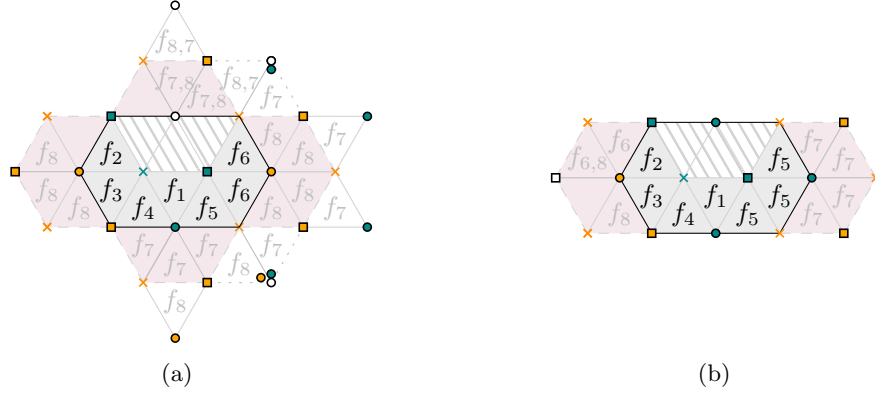


Figure 17: Illustration of the proof of Claim 11.2.

Claim 11.3. *Every polyiamond P that \triangle -contains P_Z and has size ≥ 15 folds into \mathcal{O} .*

Proof. We may assume that P does not \triangle -contain P_X nor P_U ; otherwise Claims 11.1 and 11.2 imply the statement. Consequently, P has seven triangles outside the C_{10} -frame depicted in Figure 18(a).

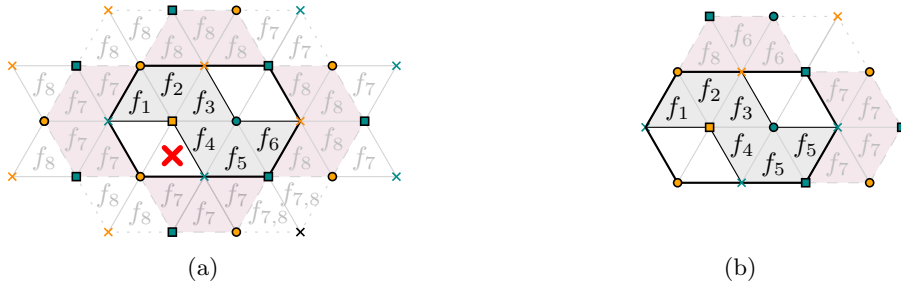


Figure 18: Illustration for the proof of Claim 11.3.

Similar as above, we consider the case that there exists a flap with a neighboring triangle outside the flap. Then, the map in Figure 18(a) induces triangles with labels f_7 and f_8 . Moreover, the depicted polyiamonds folds into \mathcal{O} and \triangle -contains P . The same argument can be applied for the case that there exist triangles in flaps with different labels.

It remains to consider the case that all triangles are contained in neighboring flaps with the same labels. By the rotational symmetry, we may assume that all triangles are contained in the top and right flap as illustrated in Figure 18(b); moreover, we know that all of these triangles are present because at least seven triangles exist outside the C_{10} -frame. The illustrated polyiamond folds into \mathcal{O} and \triangle -contains P . Thus, P folds into \mathcal{O} . \square

Claim 11.4. *Every polyiamond P that \triangle -contains P_L and has size ≥ 15 folds into \mathcal{O} .*

Proof. Observe that every triangle outside the dashed frame in Figure 19(a) yields a triangle with the missing label f_8 . Hence, we may assume that P is contained in the frame. Moreover, we may assume that P does not contain P_U nor P_Z ; otherwise Claims 11.2 and 11.3 imply the statement. Consequently, at least 3 triangles are missing within the frame as indicated, where crosses on an edge indicate that at most one of the incident triangles exist.

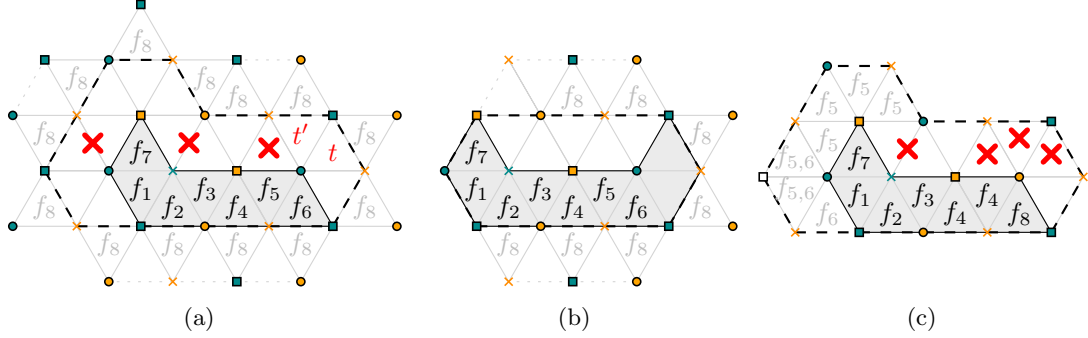


Figure 19: Illustration for the proof of Claim 11.4.

We distinguish two cases: If P contains the triangle t , then it contains the polyiamond depicted in Figure 19(b). Because the frame contains only 14 triangles, there exists a triangle f outside the frame. Together with the depicted map (or its mirror image), f ensures a triangle with label f_8 .

If P does not contain the triangle t , then its left neighboring triangle t' does not belong to P because P is contained in the dashed frame, see Figure 19(c). The frame-polyiamond depicted in Figure 19(c) has four triangles with label f_5 , one with f_6 and two with joker label $f_{5,6}$ (indicating that these can be adjusted as wished). Because P does not \triangle -contain P_Z nor P_U , at most three of the remaining triangles without labels exist. It follows that any choice of eight additional triangles contains two triangles with different labels. By adjusting the joker label as needed, these labels can represent f_5 and f_6 . Moreover, the depicted polyiamonds fold into \mathcal{O} . \square

6 Folding with Prescribed Face Coverage

For a polyiamond folded into the octahedron, we call the number of triangles covering each face its *covering number*. Clearly, the covering number is a positive integer; otherwise the polyiamond does not fold into \mathcal{O} . In this section, we aim to find polyiamonds that fold into the octahedron such that each face f_i of the octahedron is covered by an assigned positive integer m_i of triangles. We show that for each choice of assigned positive integers, there exists a foldable polyiamond such that the covering number of each face is equal to the assigned number.

Theorem 12. *Let $(m_i)_{i=[8]}$ be a sequence of positive integers. Then there exists a polyiamond P that folds into \mathcal{O} such that the covering number of face f_i is m_i .*

In particular, there exists such a polyiamond P that does neither contain holes nor slit edges.

Proof. For simplicity, we start by presenting a polyiamond with slit edges that folds into \mathcal{O} as required. Afterwards, we modify the strategy to obtain polyiamonds without slit edges.

Figure 20 displays a polyiamond that can be viewed as an octahedral net with *arms* of appropriate length. Apart from the net, each face f_i is assigned an arm A_i consisting of $m_i - 1$ triangles. Each arm can be folded on the incident triangle of the net by folding the grid edges using alternating mountain and valley folds.

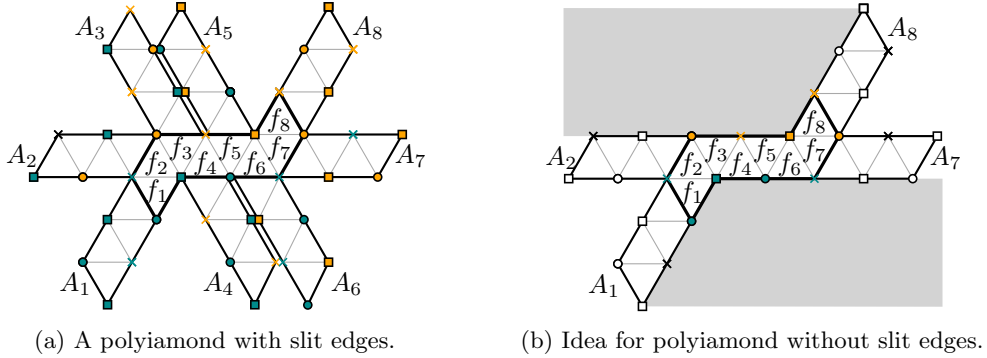


Figure 20: Illustration for the proof of Theorem 12.

In order to obtain a polyiamond without slit edges, a little more work is required. The arms A_1, A_2, A_7, A_8 remain unchanged as depicted in Figure 20(b). The idea is to attach the arm A_4 to the arm A_3 such that both arms stay within the top gray region. Symmetrically, the arm A_5 is attached to A_6 . We distinguish a few simple cases:

If $m_3 \geq 4$, then we attach the arm A_4 on A_3 as depicted in Figure 21(a). The coloring of the vertices shows that the triangle of each arm can be folded onto the correct face of \mathcal{O} .

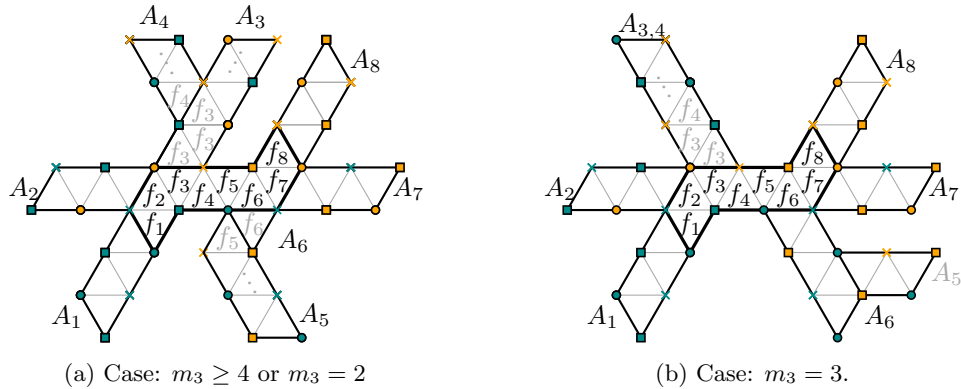


Figure 21: Illustration for the proof of Theorem 12.

Similarly, if $m_3 = 2$, we attach the arm A_4 on the right side of the arm A_3 consisting of one triangle as in Figure 21(a) (illustrated for A_5 and A_6).

If $m_3 = 3$, then we consider the polyiamond in Figure 21(b) with arm $A_{3,4}$ of length $(m_3 - 1) + (m_4 - 1)$. Note that we may fold the first two triangles onto f_3 and the remaining ones onto f_4 .

By symmetry, we handle the cases of $m_6 = 2, 3, \geq 4$ analogously. Hence, it remains to consider the case that $m_3 = 1$ or $m_6 = 1$ (or both). Note that f_3 and f_6 do not share vertices and hence, they are opposite faces. Using the symmetry of the octahedron, we may assume that f_3, f_6 is a pair of opposite faces maximizing $\min\{m_3, m_6\}$. It thus remains to consider the case that all four pairs of opposite faces contain a face with covering number 1. Either, two of these faces share an edge or there exist exactly four faces with $m_i = 1$, none of which share an edge. If two of the faces with covering number 1 share a side, we map them to f_4 and f_5 . Note that removing the arms A_4, A_5 in Figure 20(a) yields a polyiamond without slit edges. Otherwise, we may assume that $m_1 = m_3 = m_5 = m_7 = 1$ and we consider the polyiamond in Figure 22. It consists of a net and four arms that can be folded onto its respective faces as before. \square

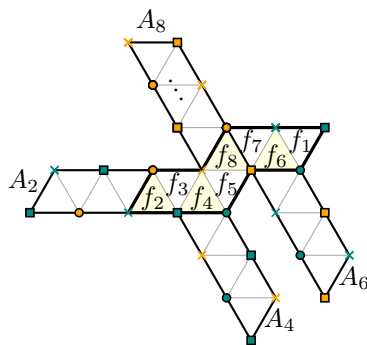


Figure 22: Illustration for the proof of Theorem 12 for the case that $m_1 = m_3 = m_5 = m_7 = 1$.

7 Future work

In this paper, we studied foldability of polyiamonds into the octahedron. For future work, it is interesting if similar results can be obtained for foldings into other platonic solids such as the dodecahedron and the icosahedron. We note that the number of nets increases rapidly: While the cube and the octahedron have 11 nets, the dodecahedron and icosahedron have 43 380 nets [10].

Acknowledgments We thank Christian Rieck for valuable suggestions on a draft of this manuscript and the anonymous reviewers for constructive feedback. Additionally, the first author thanks Tilman Stehr for his good advice concerning questions of implementation.

References

- [1] Z. Abel, E. Demaine, M. Demaine, H. Matsui, G. Rote, and R. Uehara. Common developments of several different orthogonal boxes. In *Canadian Conference on Computational Geometry (CCCG)*, 2011. available at <http://cccg.ca/proceedings/2011/papers/paper49.pdf>.
- [2] O. Aichholzer, H. Akitaya, K. Cheung, E. Demaine, M. Demaine, S. P. Fekete, L. Kleist, I. Kostitsyna, M. Löffler, Z. Masárová, K. Mundilova, and C. Schmidt. Folding polyominoes with holes into a cube. *Computational Geometry (CGTA)*, 93:101700, 2020. doi:10.1016/j.comgeo.2020.101700.
- [3] O. Aichholzer, M. Biro, E. D. Demaine, M. L. Demaine, D. Eppstein, S. P. Fekete, A. Hesterberg, I. Kostitsyna, and C. Schmidt. Folding polyominoes into (poly)cubes. *International Journal of Computational Geometry & Applications (IJCGA)*, 28:197–226, 2018. doi:10.1142/S0218195918500048.
- [4] G. Aloupis, P. K. Bose, S. Collette, E. D. Demaine, M. L. Demaine, K. Douřeb, V. Dujmović, J. Iacono, S. Langerman, and P. Morin. Common unfoldings of polyominoes and polycubes. In *Computational Geometry, Graphs and Applications (CGGA)*, pages 44–54. Springer, 2010. doi:10.1007/978-3-642-24983-9_5.
- [5] N. M. Benbernou, E. D. Demaine, M. L. Demaine, and A. Lubiw. Universal hinge patterns for folding strips efficiently into any grid polyhedron. *Computational Geometry*, page 101633, 2020. doi:10.1016/j.comgeo.2020.101633.
- [6] N. M. Benbernou, E. D. Demaine, M. L. Demaine, and A. Ovadya. Universal hinge patterns for folding orthogonal shapes. *Origami⁵: Proceedings of the 5th International Conference on Origami in Science, Mathematics and Education (OSME)*, pages 405–419, 2011.
- [7] F. Buekenhout and M. Parker. The number of nets of the regular convex polytopes in dimension ≤ 4 . *Discrete Mathematics*, 186(1):69 – 94, 1998. doi:10.1016/S0012-365X(97)00225-2.
- [8] K. Czajkowski, E. D. Demaine, M. L. Demaine, K. Eppling, R. Kraft, K. Mundilova, and L. Smith. Folding small polyominoes into a unit cube. In *Canadian Conference on Computational Geometry (CCCG)*, pages 95–100, 2020. available at <https://vga.usask.ca/cccg2020/papers/Proceedings.pdf>.
- [9] E. Hawkes, B. An, N. M. Benbernou, H. Tanaka, S. Kim, E. D. Demaine, D. Rus, and R. J. Wood. Programmable matter by folding. *Proceedings of the National Academy of Sciences*, 107(28):12441–12445, 2010. doi:10.1073/pnas.0914069107.
- [10] T. Horiyama and W. Shoji. Edge unfoldings of platonic solids never overlap. In *Canadian Conference on Computational Geometry (CCCG)*, 2011. available at <http://cccg.ca/proceedings/2011/papers/paper107.pdf>.
- [11] K. Kuribayashi, K. Tsuchiya, Z. You, D. Tomus, M. Umemoto, T. Ito, and M. Sasaki. Self-deployable origami stent grafts as a biomedical application of ni-rich tini shape memory alloy foil. *Materials Science and Engineering: A*, 419:131–137, 03 2006. doi:10.1016/j.msea.2005.12.016.
- [12] J. Mitani and R. Uehara. Polygons folding to plural incongruent orthogonal boxes. In *Canadian Conference on Computational Geometry (CCCG)*, pages 39–42, 2008. available at <http://cccg.ca/proceedings/2008/paper07.pdf>.

- [13] A. Qattawi, M. Abdelhamid, A. Mayyas, and M. Omar. Design analysis for origami-based folded sheet metal parts. *SAE International Journal of Materials and Manufacturing*, 7(2):488–498, 2014. URL: <http://www.jstor.org/stable/26268627>.
- [14] T. Shirakawa and R. Uehara. Common developments of three incongruent orthogonal boxes. *International Journal of Computational Geometry & Applications (IJCGA)*, 23(01):65–71, 2013. doi:[10.1142/S0218195913500040](https://doi.org/10.1142/S0218195913500040).
- [15] R. Uehara. A survey and recent results about common developments of two or more boxes. In *Origami⁶: Proceedings of the 6th International Meeting on Origami in Science, Mathematics and Education (OSME)*, volume 1, pages 77–84, 2014.
- [16] D. Xu, T. Horiyama, T. Shirakawa, and R. Uehara. Common developments of three incongruent boxes of area 30. *Computational Geometry (CGTA)*, 64:1–12, 2017. doi:[10.1016/j.comgeo.2017.03.001](https://doi.org/10.1016/j.comgeo.2017.03.001).